

Fast Evaluation Peanut Oil Quality by Synchronous Fluorescence Spectroscopy and Statistical Analysis

Weiwei Zhang, Riqin Lv*, Yanhui Sun, Haiyang Gu

School of Biotechnology and Food Engineering, Chuzhou University, Chuzhou, China

Email: *249541998@qq.com

How to cite this paper: Zhang, W.W., Lv, R.Q., Sun, Y.H. and Gu, H.Y. (2021) Fast Evaluation Peanut Oil Quality by Synchronous Fluorescence Spectroscopy and Statistical Analysis. *Journal of Materials Science and Chemical Engineering*, 12, 565-574.

<https://doi.org/10.4236/as.2021.125036>

Received: April 14, 2021

Accepted: May 18, 2021

Published: May 21, 2021

Abstract

Peanut oil oxidation was to monitor and quantify combining synchronous fluorescence spectroscopy and chemometrics. Peanut oil was subjected to an accelerated oxidation testing. The spectral and related chemical indicators were caught during oxidation induce testing. Fluorescence spectra were gained for each sample with simultaneous excitation from 200 to 800 nm and the offsets ($\Delta\lambda$) of 10 to 180 nm during the oxidation process. The results showed the induce period (IP) of the peanut oil was 16.45 h. Parallel factor analysis (PARAFAC) was performed to select the best $\Delta\lambda$ interval of 70 nm, which spectral data was the most suitable for interval partial least square (iPLS) and synergy interval PLS (siPLS) modeling and forecast. The study presented all interval selection methods had the better results than the global spectrum modelling. iPLS reached the best into 10 intervals with a ratio of prediction to deviation (RPD) of 2.10. siPLS that separated the whole spectrum into 15 intervals and combined the third intervals (282 to 320 nm, 362 to 400 nm, and 761 to 800 nm) had a ratio of RPD of 2.26. The results showed the optimal siPLS model performed a little better than iPLS. The established model lying on interval selection could improve the prediction accuracy. It could provide a quick, accurate method to monitor oil oxidation process.

Keywords

Synchronous Fluorescence Spectroscopy, Peanut Oil, Oxidation Stability, Chemometrics

1. Introduction

Peanut oil is one of the most sought-after edible oil in China. Oxidation of lipids also occurs in oil in the processing and storage [1]. However, the monitoring of

oil quality is a complex analytical challenge. Therefore, various detection methods have been proposed to assess the oil quality [2], such as determining the acid and peroxide values related to the oxidation state by chromatography [3], sensory evaluation [4], and physicochemical method [5]. However, most of the methods not only require expensive instruments with tedious chemical procedures but also are time-consuming and even have danger [6] [7]. Thus, a fast and non-destructive method is in high demand.

With characteristics of fast, sensitivity and simplicity, synchronous fluorescence spectroscopy has been used successfully for detection of adulteration [8] [9] and is preferable for the multivariate quantitative analysis in real-time [10]. To increase the accuracy of prediction, different chemometrics analyses have been applied to choose the spectral region of the model for optimization [11]. Principal component analysis (PCA), a multivariate projection method is used for the interpretation the differences between oil samples by scores plots of principal components [12] [13] [14]. Parallel factor analysis (PARAFAC) is a very widespread method to decompose multi-way data into their underlying chemical components [15] [16]. It had a good application in evaluating oil quality based on pattern recognition method [17]. Another matter deserving attention is interval partial least square (iPLS) and synergy interval PLS (siPLS). As reported, the two methods established model optimized by selected subinterval achieved the best prediction effect rather than the model based on full-spectrum information associated with chemical test value [18] [19] [20].

Despite the helpful evaluation ability of these detection methods for oil quality, this project was to use several methods to build a robust and reliable predictive model for monitoring changes occurring oxidation in time.

2. Experimental

2.1. Sample Preparation

Sample peanut oil purchased from a local grain and oil shop in the study. Oil samples were been heated at 90°C under oil oxidation stabilizer (VELP Oxitest, Italy) for testing. Each sample was examined for synchronous fluorescence spectroscopy and peroxide value (PV) every hour.

2.2. Fluorescence Measurements

Fluorescence landscapes were acquired by spectrofluorometer (Car Eclipse, Varian) with a 1 cm quartz cuvette. The excitation wavelengths (Ex) was ranged from 200 to 800 nm with 5 nm increments. Synchronous fluorescence spectra for each sample were collected by simultaneously scanning the excitation and the emission monochromators with different offsets ($\Delta\lambda$) from 10 to 180 nm. Spectra were recorded three times every sample.

2.3. Statistical Analysis

The synchronous fluorescence spectrum consist of three-dimensional data, fluo-

rescence intensity, excitation wavelength and $\Delta\lambda$. PARAFAC was well used to select the best $\Delta\lambda$ interval by a loading score to decompose trilinear multi-way data arrays [21].

iPLS and siPLS model were performed in order to relate the fluorescence intensity of oils with oxidation components through interval selection. In the present study, the global spectrum was sectioned into non-overlapping equidistant intervals of 10, 15, 20, 30 and 35, respectively. For siPLS, the PLS regression was applied for all possible combinations of 2, 3 and 4 subintervals, respectively. For the two established models, the optimal interval was evaluated by analyzing different factors, like the root means square error of cross-validation (RMSECV) and the ratio of prediction to deviation (RPD) [7] [22]. All analysis was conducted using the software Matlab R 2014a.

3. Results and Discussion

3.1. The Landscapes of the Fluorescence Spectrum

Figure 1 showed the effect of different oxidation time on 3D spectra of oils. The maps consisted of three parts, X-axis, Y-axis and Z-axis, which represented the excitation wavelength, the $\Delta\lambda$ interval and the fluorescence intensity, respectively. The 3D spectra often facilitated the qualitative analysis of the fluorescence patterns. From **Figure 1(a)**, the fresh peanut oil had a very high-intensity peak in the region of 20 to 150 nm and 300 to 400 nm for $\Delta\lambda$ and Ex, respectively. The peak presumably included tocopherols and phenolic antioxidants that were unstable during oxidation [23] [24]. In **Figure 1(b)**, the spectra in oxidation induce condition at 16.34 h exhibited a high-intensity change. The significant changes in the fluorescence intensity were mainly due to the first oxidation products, such as the variety of hydro-peroxide. However, oil after oxidation induce showed a relatively great change in intensity. Because the AV increased significantly

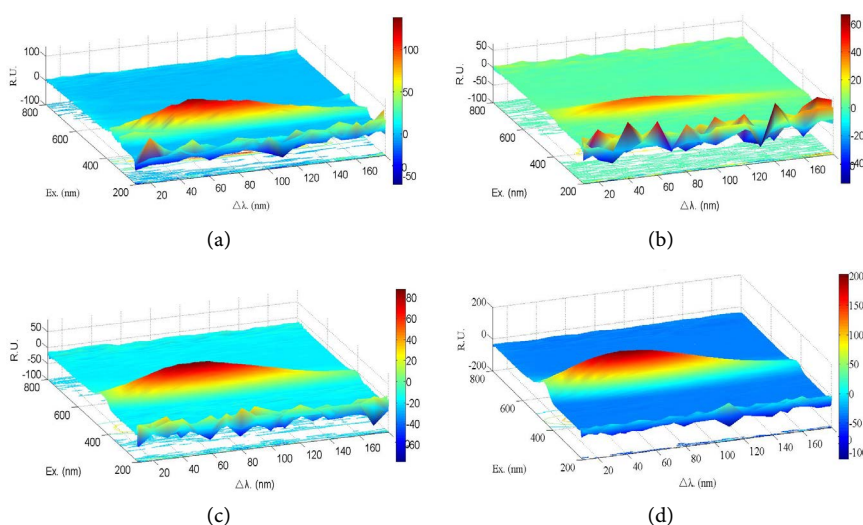


Figure 1. 3D spectra of peanut oil with different oxidation periods. (a) Fresh oil, (b) Oxidation induce period, (c) Oxidation for 24 h, (d) Oxidation for 36 h.

and formed some second-order oxidation products, e.g. ketones, aldehydes and carboxyl-compound [25] [26]. Then the color of the spectra did not deepen until stable compounds were produced by free radicals. The results showed all the changes of the synchronous fluorescence spectrum were highly correlated with the chemical parameters in the study.

3.2. PARAFAC Analysis

As reported, the PARAFAC method is a powerful tool for dealing with multi-way datasets in underlying structures [16]. The PARAFAC method was to select the optimal $\Delta\lambda$ interval. At first, the appropriate number of components must be caught with the sum of the squared error, which was shown in **Figure 2**. As in **Figure 2(a)**, the sum of the squared error for the sixth component was less than that for the fifth and seventh components. Another way, the eighth component model is also suitable for the PARAFAC algorithm. But according to previous literature reports, the fewer component (*i.e.*, 6) was much more adequate [27]. **Figure 2(b)** showed the loading score for the $\Delta\lambda$ interval values based on 6 components. The result showed the $\Delta\lambda$ interval of 70 nm had the maximum loading score.

3.3. Analysis of the Decomposed Fluorescence Spectroscopy

As shown in **Figure 3**, the spectra ($\Delta\lambda = 70$ nm) was selected by the PARAFAC method and the different regions of taking particular information for each oxidation period. Prior to oxidation (fresh oil, **Figure 3**), the excitation spectra got a very high-intensity peak near 350 nm. According to literature, this excitation band was related to tocopherol, polyphenol, which was by that detected by Gu *et al.* [1]. In oxidation induce period, the intensity of the new peak was appeared with excitation ranges from 350 to 450 nm. Signals were attributed to the continuous oxidation products. The other two areas centered at 400 to 550 nm may be produced by hydro-peroxides, which may explain the oxidation state [24]. The intensity changed are likely caused the same reason as reported by Gu *et al.* [17].

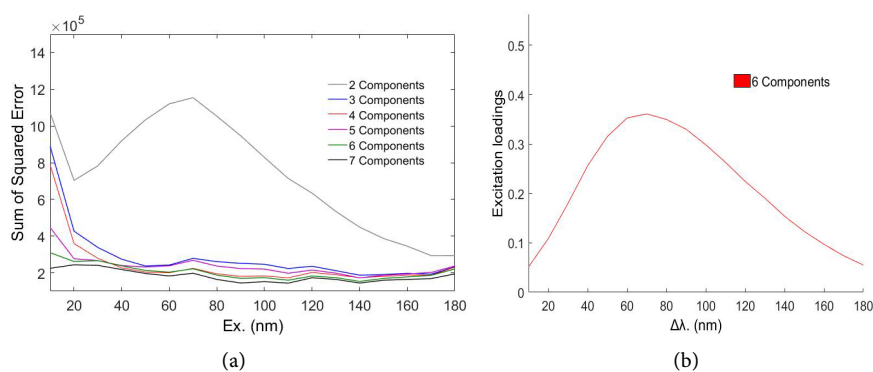


Figure 2. (a) Sum of squared error at different components, (b) Excitation loadings at different $\Delta\lambda$ interval.

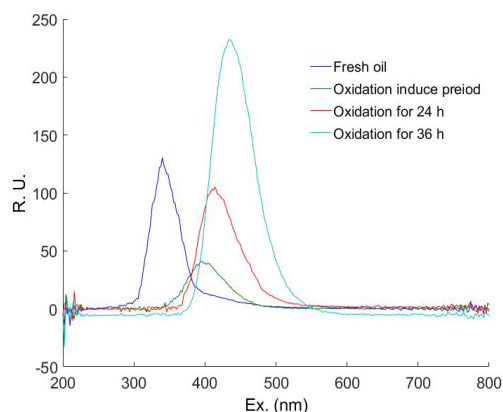


Figure 3. 2D spectrum evolution during different oxidation period.

3.4. iPLS Analysis Model

The global spectrum with 200 to 800 nm was sectioned into 10, 15, 20, 25 and 30 subintervals and the models were compared to select the best one through iPLS. **Table 1** showed all the optimal iPLS models results. From **Table 1**, the result verified the sub interval number had an impact on the iPLS modelling and the iPLS model with 10 subintervals seemed more robust. The RPD of the model was 2.10, which indicated a good quantitative model [28] [29]. Meanwhile, models with RMSEP/RMSECV below 1.2 were generally considered much more robust [30] [31].

Figure 4 showed the expected prediction error (RMSECV) of iPLS with the 10 subintervals and the global model (horizontal black line) plotted together with a normalised mean spectrum. In the figure, the heights of the rectangles represent RMSECV of PLS model in each subinterval, and the horizontal line corresponds to RMSECV of the global model. As seen in **Table 1** and **Figure 4**, each model performed better than the global model among all items. But only 4th subinterval with 10 sectioned was the best due to the lowest RMSECV of 0.392 and the selected wavelength located range 382 to 440 nm (**Table 1**). The variables corresponded well to the oxidation product, which made the result mode more interpretative.

3.5. siPLS Analysis Model

siPLS combined the same interval division as the iPLS, and the synergy interval number was set to 2, 3 and 4. The prediction results of each model were given in **Table 2**. In **Table 2**, both divisions and synergic subintervals affected siPLS model. Similarly, all models had better prediction results than the global model (**Figure 4**). Particularly, among all the resultant models, the siPLS model, divided into 15 subintervals with three subintervals [3] [5] [15] achieved the best prediction accuracy. The wavelength ranges were chosen 282 - 320 nm, 362 - 400 nm, 761 - 800 nm, respectively. Comparing the two models, the selected siPLS model was better than the optimized iPLS model above, owing to its lower RMSEP/RMSECV of 1.05 and the higher RPD 2.26.

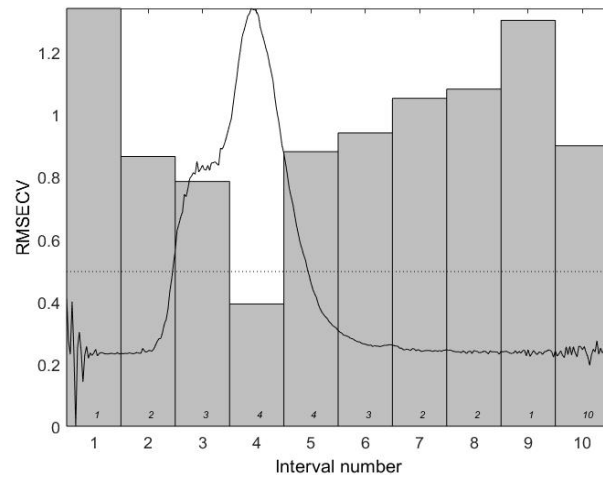


Figure 4. RMSECV for 10 interval models obtained for each local PLS model and for the global model (horizontal black line) using iPLS with latent variables (italic numbers inside rectangles).

Table 1. Quantification results form iPLS model.

| Section | PLS component | Optimal band | RMSECV | RMSEP | RMSEP/RMSECV | RPD |
|---------|---------------|--------------|--------|-------|--------------|------|
| 10 | 4 | 382 - 440 | 0.392 | 0.330 | 0.84 | 2.10 |
| 15 | 5 | 362 - 400 | 0.460 | 0.486 | 1.05 | 1.57 |
| 20 | 7 | 382 - 410 | 0.435 | 0.384 | 0.88 | 1.91 |
| 25 | 8 | 370 - 392 | 0.471 | 0.369 | 0.78 | 2.09 |
| 30 | 10 | 382 - 400 | 0.477 | 0.691 | 1.24 | 1.31 |

Table 2. Optimal results of siPLS modelling.

| Section | PLS component | Interval number | RMSECV | RMSEP | RMSEP/RMSECV | RPD |
|---------|---------------|-----------------|--------|-------|--------------|------|
| | 6 | [4 7] | 0.401 | 0.435 | 1.08 | 1.65 |
| 10 | 4 | [4 7 10] | 0.396 | 0.351 | 0.87 | 2.06 |
| | 4 | [4 7 8 10] | 0.401 | 0.346 | 0.86 | 2.18 |
| | 5 | [5 15] | 0.352 | 0.377 | 1.07 | 2.18 |
| 15 | 5 | [3 5 15] | 0.348 | 0.367 | 1.05 | 2.26 |
| | 5 | [3 5 10 15] | 0.352 | 0.365 | 1.04 | 2.18 |
| | 6 | [7 14] | 0.371 | 0.365 | 0.98 | 1.79 |
| 20 | 8 | [3 7 13] | 0.360 | 0.447 | 1.24 | 1.74 |
| | 8 | [3 7 12 13] | 0.362 | 0.449 | 1.24 | 1.49 |
| | 5 | [5 8] | 0.377 | 0.461 | 1.22 | 1.48 |
| 25 | 5 | [5 8 10] | 0.359 | 0.485 | 1.35 | 1.35 |
| | 5 | [5 8 17 20] | 0.355 | 0.484 | 1.36 | 1.34 |
| | 4 | [10 30] | 0.360 | 0.399 | 1.11 | 1.76 |
| 30 | 8 | [2 10 30] | 0.271 | 0.217 | 0.80 | 1.95 |
| | 10 | [2 4 10 30] | 0.226 | 0.275 | 1.21 | 2.04 |

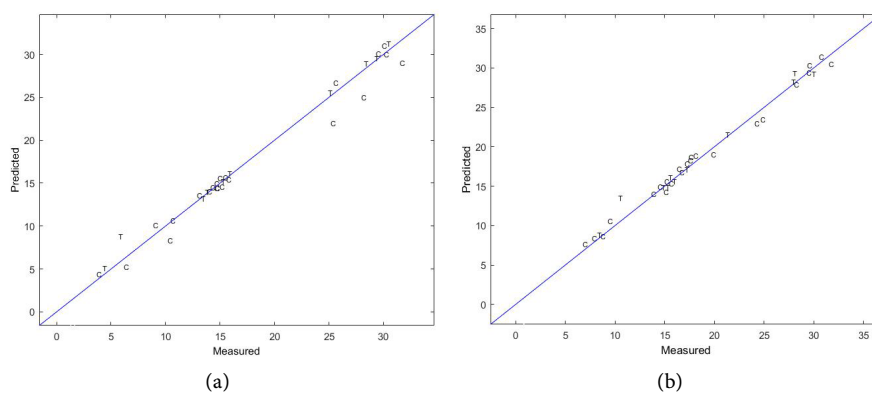


Figure 5. (a) Predicted vs measured plot for the selected iPLS model, (b) A corresponding plot from a siPLS model with 15 subdivisions optimisation. In the plot, C denotes cross-validated predictions, and T denotes the independent test set predictions.

Figure 5 showed the scatter plot of the iPLS model with 4 components and the siPLS with 15 subdivisions model in the calibration and prediction sets. Obviously, siPLS model had a closer cluster of samples along the reference line than that of iPLS model. In addition, the siPLS method was preferable when there were multiple characteristic bands related to components of the samples of interest [7].

4. Conclusion

Combined methods of fluorescence spectroscopy with chemometrics analysis acquired in the present study revealed it is feasible to evaluate the evolution of oil oxidation at any required time with fluorescence devices. Based on the synchronous fluorescence spectrum, the best $\Delta\lambda$ interval was 70 nm by PARAFAC. The spectral data dealing with PARAFAC for siPLS with 15 intervals and iPLS with 4 components achieve high prediction accuracy, respectively. The selected siPLS model with an RPD of 2.067, and the relevant band of 282 - 320 nm, 362 - 400 nm, 761 - 800 nm. For iPLS model had the RPD of 2.07 and extracted the band of 380 - 440 nm. siPLS outperformed iPLS modelling because the former had a higher RPD and captured more relevant variables. The results suggest the proposed model is well used to monitor oil oxidation in time. Furthermore, the future work is the validation of the methodology with variety of oil samples to provide a more reliable model.

Acknowledgements

The authors acknowledge funding by the National Natural Science Foundation of China (31701685), Anhui Natural Science Foundation (1608085MC73), Anhui Postdoctoral Foundation (2019B362), Anhui Postdoctoral Science (Chuzhou University) Foundation (2020BSH002).

Conflicts of Interest

The authors declare no conflicts of interest regarding the publication of this paper.

References

- [1] Gu, H.Y., Sun, Y.H. and Lv, R.Q. (2019) A Feasibility Study for Rapid Evaluation of Oil Quality Undergoing Oven Treatment Using Synchronous Fluorescence Spectrum. *Chem Paper*, **73**, 1953-1959. <https://doi.org/10.1007/s11696-019-00748-3>
- [2] Geng, D.C., Chen, B. and Chen, M.J. (2019) Polarization Perturbation 2D Correlation Fluorescence Spectroscopy of Edible Oils: A Pilot Study. *J Food Meas Charact*, **13**, 1566-1573. <https://doi.org/10.1007/s11694-019-00072-0>
- [3] Belichovska, D., Hajrulaimusliu, Z., Uzunov, R., Belichovska, K. and Arapcheska, M. (2015) Fatty Acid Composition of Ostrich (*Struthio camelus*) Abdominal Adipose Tissue. *Mac Vet Rev*, **38**, 53-59. <https://doi.org/10.14432/j.macvetrev.2014.11.028>
- [4] Aladedunye, F. (2016) Toxic Contaminants of Thermos-Oxidatively Processed Edible Oils/Fast. *Lipid Technol*, **28**, 117-121. <https://doi.org/10.1002/lite.201600032>
- [5] Cao, J., Li, C., Liu, R., Liu, X.R., Fan, Y.W. and Deng, Z.Y. (2017) Combined Application of Fluorescence Spectroscopy and Chemometrics Analysis in Oxidative Deterioration of Edible Oil Oils. *Food Anal Methods*, **10**, 649-658. <https://doi.org/10.1007/s12161-016-0587-2>
- [6] Dankowska, A. and Kowalewski, W. (2019) Comparison of Different Classification Methods for Analysing Fluorescence Spectra to Characterise Type and Freshness of Olive Oils. *Eur Food Res Technol*, **245**, 745-752. <https://doi.org/10.1007/s00217-018-3196-z>
- [7] Lu, Y.Z., Du, C.W., Yu, C.B. and Zhou, J.M. (2014) Fast and Nondestructive Determination of Protein Content in Rapeseeds (*Brassica napus* L.) Using Fourier Transform Infrared Photoacoustic Spectroscopy (FTIR-PAS). *J Sci Food Agric*, **94**, 2239-2245. <https://doi.org/10.1002/jsfa.6548>
- [8] Kunz, M.R., Ottaway, J., Kalivas, J.H., Georgiou, C.A. and Mousdis, G.A. (2011) Updating a Synchronous Fluorescence Spectroscopic Virgin Olive Oil Adulteration Calibration to a New Geographical Region. *J Agric Food Chem*, **59**, 1051-1057. <https://doi.org/10.1021/jf1038053>
- [9] Ge, F., Chen, C., Liu, D. and Zhao, S. (2014) Rapid Quantitative Determination of Walnut Oil Adulteration with Sunflower Oil Using Fluorescence Spectroscopy. *Food Anal Methods*, **7**, 145-150. <https://doi.org/10.1007/s12161-013-9610-z>
- [10] Jin, H., Hwang, S.J. and Shin, J.K. (2008) Using Synchronous Fluorescence Technique as a Water Quality Monitoring Tool for an Urban River. *Water Air Soil Pollut*, **191**, 231-243. <https://doi.org/10.1007/s11270-008-9620-4>
- [11] Li, Y.P., Fang, T., Zhu, S.Q., Huang, F.R., Chen, Z.Q. and Wang, Y. (2017) Detection of Olive Oil Adulteration with Waste Cooking Oil via Raman Spectroscopy Combined with iPLS and SiPLS. *Spectrochim Acta A (MBS)*, **189**, 37-43. <https://doi.org/10.1016/j.saa.2017.06.049>
- [12] Aguado, D., Montoya, T., Borrás, L., Seco, A. and Ferrer, J. (2008) Using SOM and PCA for Analysing and Interpreting Data from a P-Removal SBR. *Eng Appl Artif Intell*, **21**, 919-930. <https://doi.org/10.1016/j.engappai.2007.08.001>
- [13] Sikorska, E., Gliszczynska-Swiglo, A., Khmelinskii, I. and Sikorski, M. (2005) Synchronous Fluorescence Spectroscopy of Edible Vegetable Oils. Quantification of tocopherols. *J Agric Food Chem*, **89**, 217-225. <https://doi.org/10.1016/j.foodchem.2004.02.028>
- [14] Lia, F., Morote-Castellano, A., Zammit-Mangion, M. and Farrugia, C. (2018) Application of Fluorescence Spectroscopy and Chemometric Models for the Detection

- of Vegetable Oil Adulterants in Maltese Virgin. *J Food Sci Technol*, **55**, 2143-2151. <https://doi.org/10.1016/j.foodchem.2004.02.028>
- [15] Valderrama, P., Marco, P.H., Lccquet, N., Ammari, F. and Rutledge, D.N. (2011) A Procedure to Facilitate the Choice of the Number of Factors in Multi-Way Data Analysis Applied to the Natural Samples: Application to Monitoring the Thermal Degradation of Oils Using Front-Face Fluorescence Spectroscopy. *Chemom Intel Lab Syst*, **106**, 166-172. <https://doi.org/10.1016/j.chemolab.2010.05.011>
- [16] Kathleen-Murphy, R., Colin-Stedmon, A., Daniel, G. and Rasmus, B. (2013) Fluorescence Spectroscopy and Multi-Way Techniques PARAFAC. *Anal Methods*, **5**, 6557-6566. <https://doi.org/10.1039/c3ay41160e>
- [17] Gu, H.Y., Sun, Y.H., Liu, S.L., Li, S.F. and Zhang, W.W. (2018) A Feasibility Study of the Rapid Evaluation of Oil Oxidation Using Synchronous Fluorescence Spectroscopy. *Food Anal Methods*, **11**, 3464-3470. <https://doi.org/10.1007/s12161-018-1315-x>
- [18] Norgaard, L., Saudland, J., Wagner, J., Nhelsen, J.P., Munck, L. and Engelsen, S.B. (2000) Interval Partial Least-Squares Regression (iPLS): A Comparative Chemometric Study with an Example from Near-Infrared Spectroscopy. *Appl Spectrosc*, **54**, 413-419. <https://doi.org/10.1366/0003702001949500>
- [19] Chen, Q.S., Zhao, J.W., Liu, M.H., Cai, J.R. and Liu, J.H. (2008) Determination of Total Polyphenols Content in Green Tea Using FT-NIR Spectroscopy and Different PLS Algorithms. *Journal of Pharmaceutical and Biomedical Analysis*, **46**, 568-573. <https://doi.org/10.1016/j.jpba.2007.10.031>
- [20] Delfino, I., Camerlingo, C., Portaccio, M. and Bartolomeo, D.V. (2011) Visible Micro-Raman Spectroscopy for Determining Glucose Content in Beverage Industry. *Food Chem*, **127**, 735-742. <https://doi.org/10.1016/j.foodchem.2011.01.007>
- [21] Sahar, A., Boubellouta, T., Portanguen, S., Kondjoyan, A. and Dofour, E. (2009) Synchronous Front-Face Fluorescence Spectroscopy Coupled with Parallel Factors (PARAFAC) Analysis to Study the Effects of Cooking Time on Meat. *J Food Sci*, **74**, E534-E539. <https://doi.org/10.1111/j.1750-3841.2009.01365.x>
- [22] Abbas, K., Karoui, R. and At-Kaddour, A. (2012) Application of Synchronous Fluorescence Spectroscopy for the Determination of Some Chemical Parameters in PDO French Blue Cheeses. *Eur Food Res Technol*, **234**, 457-465. <https://doi.org/10.1007/s00217-011-1652-0>
- [23] Sayago, A., Morales, M.T. and Aparicio, R. (2004) Detection of Hazelnut in Virgin Olive Oil by a Spectrofluorimetric Method. *Eur Food Res Technol*, **218**, 480-483. <https://doi.org/10.1007/s00217-004-0874-9>
- [24] Kyriakidis, N.B. and Skarkalis, P. (2000b) Fluorescence Spectra Measurement of Olive Oil and Other Vegetable Oils. *J AOAC Int*, **83**, 1435-1439. <https://doi.org/10.1093/jaoac/83.6.1435>
- [25] Hao, X., Li, J. and Yao, Z. (2016) Changes in PAHs Levels in Deible Oils during the Deep-Frying Process. *Food Control*, **66**, 233-240. <https://doi.org/10.1016/j.foodcont.2016.02.012>
- [26] Taghvaei, Z., Piracicaniak, Z., Razari, K. and Faraji, M. (2016) Determination of Polycyclic Aromatic Hydrocarbons (PAHs) in Olive and Refined Pomace Olive Oils with Modified Low Temperature and Ultrasound-Assisted Liquid-Liquid Extraction Method Followed by the HPLC/FLD. *Food Anal Methods*, **9**, 1220-1227. <https://doi.org/10.1007/s12161-015-0297-1>
- [27] Stedmon, C.A. and Bro, R. (2008) Characterizing Dissolved Organic Matter Fluorescence with Parallel Factor Analysis: A Tutorial. *Limnol Oceanogr Methods*, **6**,

- 572-579. <https://doi.org/10.4319/lom.2008.6.572>
- [28] Williams, C. and Sobering, D.C. (1993) Comparison of Commercial Near Infrared Transmittance and Reflectance Instruments for Analysis of Whole Grains and Seeds. *J Near Infrared Spectrosc*, **1**, 25-32. <https://doi.org/10.1255/jnirs.3>
- [29] Viscarra-Rossel, R.A., McGlynn, R.N. and McBratney, A.B. (2006) Determination the Composition of Mineral-Organic Mixes Using UV-Vis-NIR Diffuse Reflectance Spectroscopy. *Geoderma*, **137**, 70-82. <https://doi.org/10.1255/jnirs.3>
- [30] Couteaux, M.M., Sarmiento, L., Herve, D. and Acevedo, D. (2005) Determination of Water-Soluble and Total Extractable Polyphenolics in Biomass, Necromass and Decomposing Plant Material Using Near-Infrared Reflectance Spectroscopy (NIRS). *Soil Biol Biochem*, **37**, 795-799. <https://doi.org/10.1016/j.soilbio.2004.08.028>
- [31] Ana, A., Antonio, S., Philippe, R., Luc, E.P., Jwan-Paul, C. and Manfred, S. (2012) A Common Near Infrared-Based Partial Least Squares Regression Model for the Prediction of Wood Density of *Pinus pinaster* and *Larix eurolepis*. *Wood Sci Technol*, **46**, 157-175. <https://doi.org/10.1007/s00226-010-0383-x>